
Rethinking Learned Image Compression: Context is All You Need

Jixiang Luo *
jixiangluo85@gmail.com

Abstract

Since LIC has made rapid progress recently compared to traditional methods, this paper attempts to discuss the question about 'Where is the boundary of Learned Image Compression(LIC)?' with regard to subjective metrics. Thus this paper splits the above problem into two sub-problems: 1) Where is the boundary of rate-distortion performance of PSNR? 2) How to further improve the compression gain and achieve the boundary? Therefore this paper analyzes the effectiveness of scaling parameters for encoder, decoder and context model, which are the three components of LIC. Then we conclude that scaling for LIC is to scale for context model and decoder within LIC. Extensive experiments demonstrate that overfitting can actually serve as an effective context. By optimizing the context, this paper further improves PSNR and achieves state-of-the-art performance, showing a performance gain of 14.39% with BD-RATE over VVC.

1 Introduction

The exponential growth of digital imagery in recent years has driven the need for efficient storage and transmission solutions, while traditional methods like JPEG [76], BPG [5], WebP [64] can not meet the demands. With the proliferation of high-resolution cameras and the widespread adoption of multimedia applications, the size of image data has surged, presenting significant challenges in terms of storage capacity and bandwidth requirements. Traditional image compression techniques, such as JPEGXL [3] including lossy and lossless JPEG recompression, AVIF [4] extracted from AV1 [14], HEIF [39] extracted from HEVC [71], have been the cornerstone of addressing these challenges. However, these methods often struggle to achieve the desired balance between compression efficiency and preservation of image quality. While these approaches have theoretical and mathematical explanations, they are all based on handcrafted designs of individual modules, lacking joint optimization of objectives to achieve an optimal Pareto frontier. Additionally, they fail to meet the increasing demands for higher image quality, such as lower bit rates and higher objective and subjective image quality.

In response to these challenges, deep learning-based image compression techniques have emerged as a promising alternative. By harnessing the power of neural networks, these methods offer several advantages over traditional compression algorithms. Deep learning-based approaches, which encompass **encoder, decoder, quantization and context model**, have demonstrated remarkable progress in recent years, significantly advancing the state-of-the-art in image compression. This paper comprehensively reviews the progress of LIC, provides intuitive theoretical explanations, and explores the boundaries of LIC objective quality. One of the key advancements in deep learning-based image compression is the incorporation of encoder and decoder architectures. The encoder component compresses the input image into a latent representation, while the decoder component reconstructs the original image from this representation. Additionally, context models are employed to capture high-level semantic information, ensuring that important features are preserved during the compression

*Work done at Sensetime Research

Table 1: The rate-distortion performance of DCVC-FM [46] and ELIC [26] on HEVC-B sequences [9] with PSNR in RGB colorspace. I and P are the frame types defined by DCVC-FM, while ELIC takes all frames as image or I frames

methods	type		BQTerrace	BasketballDrive	Cactus	Kimono	ParkScene
DCVC-FM	I	bpp	0.0362	0.0156	0.0255	0.0157	0.0165
		PSNR	28.7238	33.6617	30.0544	33.0646	30.2771
	P	bpp	0.0007	0.0015	0.0011	0.0011	0.0008
		PSNR	29.2897	29.3356	28.8999	30.5414	28.8406
ELIC	I	bpp	0.0201	0.0096	0.0136	0.0090	0.0085
		PSNR	25.7859	29.7820	26.8106	29.9608	27.6546
	P	bpp	0.0193	0.0109	0.0133	0.0089	0.0089
		PSNR	26.1313	29.1154	26.7629	30.1376	27.2406
ELIC	I	bpp	0.1757	0.0487	0.1043	0.0618	0.1018
		PSNR	32.1260	33.4375	30.4493	34.0548	30.0388
	P	bpp	0.1609	0.0592	0.1047	0.0590	0.1100
		PSNR	32.4425	32.6736	30.4104	34.1136	30.0649

process. The backbone of LIC, comprising the encoder and decoder, primarily consists of several distinct architectural components, including convolutional neural networks (CNNs) [42, 58, 2, 28, 55, 44], recurrent neural networks (RNNs) [74, 32, 73, 49], transformers [77, 53, 51, 35, 33], and frequency decomposition methods [45, 16, 83, 24, 52]. Despite the variety of structures available, the current trend indicates that higher complexity leads to greater compression gains. Correspondingly, most solutions tend to be associated with transformers to some extent. However, combining CNNs with transformers remains the optimal approach [45, 51]. However, the difference lies in the usage: the former employs transformers in the context, while the latter integrates them into the backbone. Both approaches can enhance performance, but they also introduce varying degrees of computational complexity. Due to the high complexity of transformers in the backbone, some papers focus on optimizing the context module specifically [44, 47, 81, 28, 59, 26]. This optimization can significantly enhance the performance of the entire LIC community with great efficiency. The most crucial aspect involves modeling the relationships between latents with spatial and channel dimensions. Currently, the prevailing approach is to simulate the distribution of latents based on conditional probability, thereby obtaining the conditional entropy of latents. The boundary of conditional entropy is closely related to the selection of conditions. Hence, we cannot accurately estimate the performance boundary of LIC. Given two variables \mathcal{X}, \mathcal{Y} , we have $H(\mathcal{Y}|\mathcal{X}) < H(\mathcal{Y})$, where $H(*)$ is the entropy of variables. $H(\mathcal{Y}|\mathcal{X}) \sim \frac{H(\mathcal{Y})}{\rho(\mathcal{X}, \mathcal{Y})}$. The conditional entropy is related to the correlation ρ between two variables. If the correlation between two variables is higher, the conditional entropy will be smaller, and vice versa.

Therefore, we define pixel level, structure level, and semantic level to discuss the compression limits of LIC. At the structure level, the overall contours or edges of the image are maintained consistently with the ground truth, while other areas can vary, thus improving the compression rate. A deeper level of semantic abstraction involves an overall understanding of the image, enabling unimaginable compression levels. For example, consider compressing an image with a clean background and a running Shiba Inu. The pixel level focuses on every pixel, the structure level focuses on the outline of the dog, but the semantic level abstracts it into a single sentence. Since this sentence requires only a few bytes of storage, it achieves extreme semantic compression. Since the structure level and semantic level can be attributed to fields such as image generation [62, 19] and image understanding [20, 6], and supervised generation faces other issues such as fidelity, which are beyond the scope of this discussion, the limits discussed in this paper are confined to the pixel level only.

In addition to the encoder and decoder, quantization is also a significant consideration. On one hand, entropy coders require a fixed finite symbol set, and on the other hand, quantization is an effective means of lossy compression to increase gains. This mainly involves scalar quantization [11, 84, 67] and vector quantization [25, 38, 82]. After quantization, entropy coding is performed. Since entropy coding is a non-differentiable process, estimating the mean and variance during training and then using a Gaussian distribution to estimate the training bitrate is necessary. This is because the Gaussian distribution is the maximum entropy distribution [60, 50] constrained by the mean and variance, and it can be computed conveniently and quickly. Under the same constraints, the Laplace distribution

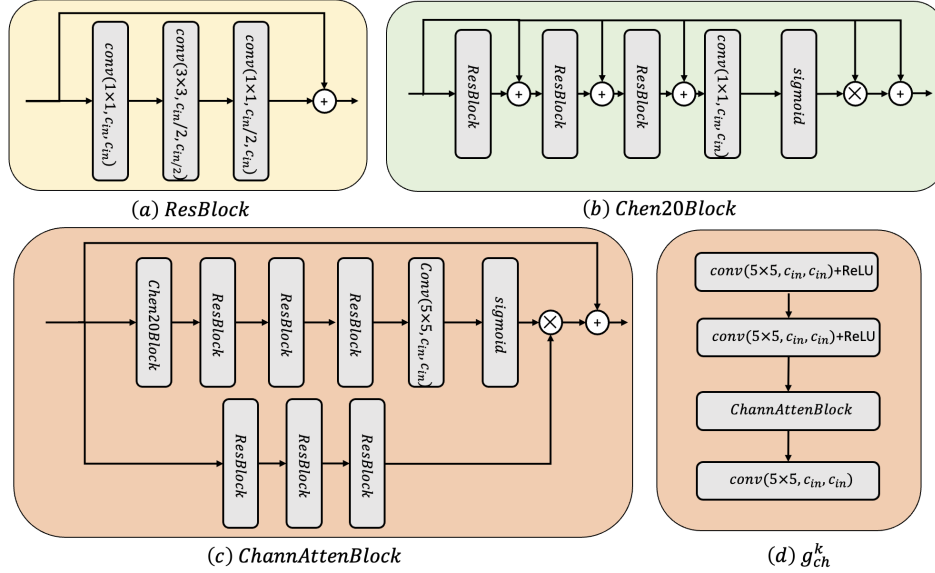


Figure 1: Channel attention for context model. 1×1 , 5×5 are the kernel size of convolutional layer, ReLU and softmax are the activation function. c_{in} is the number of input channel

also constrains the mean and variance, but its variance must be even. Its constraint property is slightly stricter than that of the Gaussian distribution. However, in some experiments, the Laplace distribution does not perform better than the Gaussian distribution even Logistic distribution in Fig.4 of [58].

By further extending the dimensions of LIC, we can obtain a broader Pareto optimization frontier, encompassing **rate-distortion-perceptuality-performance-practicality(RDPPP)**, where perceptuality means subjective quality, performance includes some downstreaming task matrices(accuracy, precision, recall), and practicality includes model size, memory and GPU occupancy, runtime speed, codec compatibility, among other factors. Since the boundary of PSNR cannot be accurately explored, another important direction is the optimization of the subjective quality [27, 56, 57, 61, 1] and integration with downstream tasks [12, 15, 21, 31, 36, 78, 54, 23, 40, 41, 69] in LIC. Researchers have been exploring the Pareto frontier of related studies from various dimensions to approach the limits of LIC. [8] exploits the Rate-Distortion-Perception, and [80] considers the practicality with regard to speed and hardware utility. Yet, from an information theory perspective, determining an upper bound for the conditional entropy of images remains elusive due to their inherent smoothness and low-rank nature. This complexity underscores the intricate nature of the problem and highlights the need for comprehensive approaches to push the performance boundary of LIC. However, due to the complexity of models and computational costs, it has been challenging to deploy LIC at both the edge and cloud devices. Therefore, while ensuring the performance of LIC, model simplification is also an important direction to consider. [48] deployed efficient decoder to improve decoder speed. [80, 75] utilizes much more engineering optimization methods. [22, 68, 66, 63] quantized full network to reduce calculations. To further simplify the model, LIC is evolved from a single-rate model to a variable-rate model, allowing one model to cover low, medium, and high-rate points [73, 17, 35, 13, 65, 70, 34, 43].

However, subjective quality, performance with downstreaming task and practicality, being a challenging aspect to quantify, are beyond the scope of this paper, which only emphasize encoder, decoder, quantization and context model. This paper seeks to address the objective metric boundary (PSNR) of LIC by integrating the analysis of scaling laws [30, 10, 29] to explore their impact on LIC. The scaling law includes number of parameters, dataset size, computing cost, loss. While increasing the training dataset and model parameters does not necessarily produce significant improvements in LIC. Therefore, this paper explores the performance of LIC by expanding the number of channels to increase model capacity, with a particular focus on examining the effects of overfitting in the context of dataset expansion.

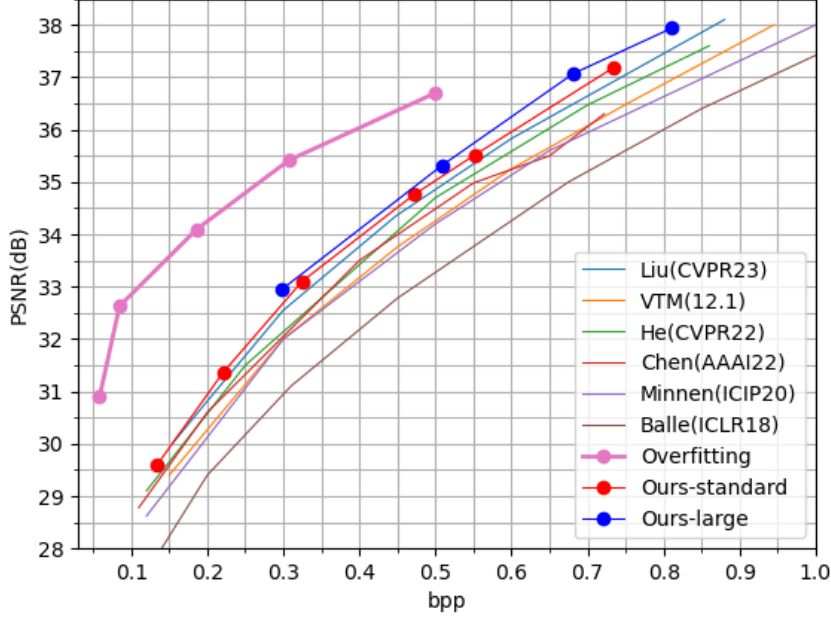


Figure 2: PSNR of Kodak dataset."Overfitting" means models trained at Kodak dataset.

Table 2: BD-RATE and BD-PSNR [7] over VTM-12.1 at Kodak dataset

%	Ours-large	Ours	Liu(CVPR23)	He(CVPR22)	Chen(AAAI22)	Minnen(ICIP20)
BD-RATE	16.91	-14.39	-11.06	-6.87	-4.09	1.43
BD-PSNR	93.12	69.22	54.12	31.02	17.96	-6.36

2 Problem Formatting

ELIC [26] utilizes a convolutional-based encoder and decoder, along with both intra-channel and inter-channel context modeling. Specifically, the channels are unevenly divided into five groups, where the earlier groups serve as the context for the later ones. Within each group, a checkerboard pattern is employed so that one subset of the checkerboard serves as the context for the other subset. This approach ensures a balance between computational complexity and compression performance gains. To further discuss this problem, we simplify the process following [54]:

$$\begin{aligned}
 \hat{y} &= Q(y) = Q(g_a(x)) \\
 \hat{x} &= g_s(\hat{y}) \\
 \hat{z} &= Q(z) = Q(h_a(x)) \\
 p &= h_s(\hat{z})
 \end{aligned} \tag{1}$$

, where g_a, g_s, h_a, h_s are the neural network parameters with encoder, decoder, the hyper-encoder and hyper-decoder at context model. Q is the quantization. The internal feature are y, z and p , and x is the input image.

$$\begin{aligned}
 \mathcal{B} &= AE_1(\hat{y}) + AE_2(\hat{z}) \\
 AE_1 &\sim [p, ctx(y, p)]
 \end{aligned} \tag{2}$$

, $AE_{1,2}, \mathcal{B}$ are arithmetic coding and bitstream. The main bitstream is from y with AE_1 , so the most crucial aspect is modeling the data distribution to accurately predict the probability of y from the

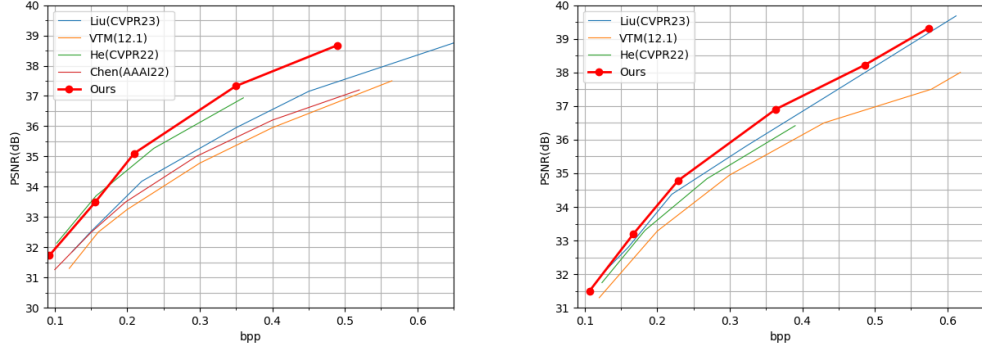


Figure 3: left:PSNR of CLIC Professional dataset. right:PSNR of Technick dataset.

aspect of data compression, achieving optimal compression rates. Hence, ctx serves as the context model to analyze p and y , ultimately providing the probabilities used by the AE_1 entropy coder. Thus h_a, h_s, ctx are called hyper context.

This paper separately evaluates the performance of increasing parameters for encoder, decoder and context model. We first discuss the ineffectiveness of scale for encoder, and then analyze its impact of parameter scales. However scales at decoder and context model is far from scaling law in large language model.

3 Motivation

DCVC-FM [46] differs from encoding P-frame residuals in that it uses the I-frame as a context to probabilistically model the P-frame. As shown in the Tab. 1, the bit-rate of the P-frame is less than one-tenth of the I-frames. For the BQTerrace sequence, the P-frame achieves a higher PSNR than the I-frame at a bit rate of one two-thousandth, due to the relatively slow motion and similar background, allowing the entire I-frame to serve as a reference for the P-frame. This significantly reduces the bit rate. However, for other videos with intense motion, while the P-frame bit rate decreases, the PSNR also correspondingly decreases. On the other hand, if a single frame image has a bit rate below $0.001bpp$, its PSNR drops well below 28 dB. These observations indicate that context is crucial for compression. To further compare, this paper uses ELIC to encode the remaining P-frames. It is evident that even with strong contextual representation, its performance is significantly inferior to the P-frame encoding in DCVC-FM. Specifically, in the BQTerrace sequence, DCVC-FM achieves $29dB$ at a bit rate of $0.0007bpp$, while ELIC requires a bit rate of $0.019bpp$ to achieve only $26dB$. Moreover, the remaining sequences in Tab. 1 have the same trend. This further illustrates that **context is all you need**.

4 Methods

This paper adopts the structure with ELIC [26], with the modification of g_{ch}^k , where k is the group of $y = g_a(x)$ split by the channel dimension. This paper introduces a plug-and-play module *ChannAttenBlock* into g_{ch}^k to enhance the context model as shown in Fig. 1. Besides this paper also combines adaptive exponential quantization following [56] with $y_{frac} = e^{(y_{frac}+a)*b} + c$, where y_{frac} is the fractional part of y , and $step$ can control the extent of quantization, which can determine the number of constant a, b, c . the larger the step size, the higher the probability that the quantized value will be zero. And here is simple implementation Coding List 1, a plugin can be plug-and-play for any LIC models, and k is the index of channel group.

Table 3: The rate distortion with increase M of encoder and decoder

M	192	384	768	1536
bpp	0.3881	0.3911	0.3834	0.3764
PSNR	33.3167	33.4058	33.4032	33.2826

4.1 Scaling for Encoder

$$\mathcal{L} = \mathcal{R} + \lambda \mathcal{D} \quad (3)$$

$$y^i = \sigma(w^i y^{i-1})$$

Code Listing 1: The implementation of adaptive exponential quantization

```

1 #input: y_i, upper_bound, step, k
2 #output: y_o
3 def quantize(y_i, upper_bound=0.5, step=0.04, i=k):
4     bias = upper_bound - step * i
5     exp_half_b = (1. + np.sqrt(1 - 4*bias*(1-bias))) / (2*bias)
6     exp_b = exp_half_b ** 2
7     constant_b = np.log(exp_b)
8     exp_ab = 1 / (exp_b - 1)
9     ab = np.log(exp_ab)
10    constant_a = ab / constant_b
11    constant_c = - np.exp(constant_a * constant_b)
12    y_frac = torch.frac(y_i)
13    y_round = y_i - y_frac
14    y_frac_flag = torch.where(y_frac >= 0, 1., -1.)
15    y_frac = torch.abs(y_frac)
16    y_frac = torch.exp((y_frac + constant_a) * constant_b) + constant_c
17    y_frac *= y_frac_flag
18    y_o = y_round + y_frac
19    return y_o

```

More experiments demonstrate that enlarging encoder makes a little difference to improve compression gain as shown in Tab. 3. Here is the training loss function for LIC, and we define the non-linear process in neural network: $\mathcal{L}, \mathcal{R}, \mathcal{D}$ are the total loss, the bit-rate and the reconstruction loss. λ is the Lagrange multiplier to balance the bit-rate and reconstruction loss. To simplify the process of gradient propagation, we define the input of i_{th} neural network layer with weight w^i as y^{i-1} , which is the output of $i-1_{th}$ layer, besides σ is the non-linear activation function. Thus we get the final output of whole neural network of LIC as L is the last layer, and $y^o = y = g_a(x)$ which is the output of encoder, where we will restrict the bit-rate, here we neglect the affect of round operation for y^o . For decoder g_s we have the following relationship:

$$\frac{\partial \mathcal{L}}{\partial w^i} = \lambda \left\langle \frac{\partial \mathcal{L}}{\partial y^L}, y^{i-1} \frac{\partial y^L}{\partial y^i} \mathcal{J}^i \right\rangle = \lambda \left\langle \frac{\partial \mathcal{D}}{\partial y^L}, y^{i-1} \frac{\partial y^L}{\partial y^i} \mathcal{J}^i \right\rangle \quad (4)$$

$$\mathcal{J}^i = \text{diag}(\sigma'(w_1^i y^{i-1}), \dots, \sigma'(w_d^i y^{i-1}))$$

For encoder g_a we have the similar formulation:

$$\frac{\partial \mathcal{L}}{\partial w^i} = \frac{\partial \mathcal{R}}{\partial w^i} + \lambda \left\langle \frac{\partial \mathcal{D}}{\partial y^L}, y^{i-1} \frac{\partial y^L}{\partial y^i} \mathcal{J}^i \right\rangle \quad (5)$$

$$= \left\langle \frac{\partial \mathcal{R}}{\partial y^o}, y^{i-1} \frac{\partial y^o}{\partial y^i} \mathcal{J}^i \right\rangle + \lambda \left\langle \frac{\partial \mathcal{D}}{\partial y^L}, y^{i-1} \frac{\partial y^L}{\partial y^i} \mathcal{J}^i \right\rangle$$

\mathcal{R} does not influence the representation of weight in g_s but affects the weight in g_a . Thus when we increase the parameter of encoder g_a under the certain bit-rate, the information bottleneck may restrict the capability of g_a , especially for the low bit-rate, which only need less feature to reconstruct the whole image. To further uncover the mechanism we depict the target and result of

Table 4: The rate-distortion for scaling of context of GFLOPS with 1920×1080 resolution

GFLOPS	channels	128	360	620	1024	1280
backbone	g_a	933.78	943.81	962.30	1,006.24	1,043.67
	g_s	933.78	943.81	962.30	1,006.24	1,043.67
hyper context	h_a	8.23	14.72	22.00	33.31	40.48
	h_s	16.68	35.09	55.71	87.75	108.06
	ctx	140.98	198.23	262.39	362.08	425.25
hyper context ratio(%)		8.16	11.61	15.02	19.36	21.56
bpp		0.5498	0.5504	0.5226	0.5131	0.5089
PSNR(dB)		35.4269	35.5509	35.7491	35.4612	35.3188

entropy optimization. Here $y^o = g_a(x)$ is the symbol to be encoded, which is subject to Gaussian distribution:

$$f(y^o) = \frac{1}{\sqrt{2\pi}\sigma} e^{-\frac{(y^o - \mu)^2}{2\sigma^2}} \quad (6)$$

$$p(\hat{y}^o) \sim p(y^o) = \int_{\hat{y}^o - 0.5}^{\hat{y}^o + 0.5} f(y^o) dy^o \quad (7)$$

μ, σ is the mean and variance of symbol y^o , $p(*)$ is the probability function of maximum entropy distribution with constrains mean μ and variance σ .

$$\begin{aligned} \mu &= h_s(\hat{z})[0] \rightarrow y^o \\ \sigma &= h_s(\hat{z})[1] \rightarrow 0 \end{aligned} \quad (8)$$

[0], [1] means μ, σ are share the input and trainable parameters, and divide the final output into two layers evenly, with the first layer being the mean and the second layer being the variance. When we optimize the object of bit-rate, we try to minimize bit-rate, $\mathcal{R} = -\log p(y^o)$, $\min \mathcal{R} \rightarrow \max p(y^o)$, namely we meanwhile minimize the scale or the dynamic range of y^o , or minimize the value of variance σ , which means y^o has less probability to obtain the value close to μ .

Thus quantization is an efficient method to improve compression gain by choosing the important information to balance the bit-rate and distortion as shown in the right of Fig. 5.

4.2 Scaling for Decoder

Decoder-only structure is to reconstruct or generate the input information. For large language model, generation is the key, and its range of output has a myriad of possibilities. Thus the scaling law can control the performance of large language model. However for LIC reconstruction has higher priority than generation. Different from in-context learning [79] at large language model, the varieties of output in LIC is constrained by y^o . But the reconstruction pixel is shift from the input pixel, reconstruction can be regarded as the restricted generation process. Thus the output space of LIC is also large but rather less than the space of large language model, which can generate new objects or scenes. The number of parameter in decoder g_s is vital for reconstruction or generation, but beyond of the discussion of this paper.

4.3 Scaling for Context

Context model is the bridge between encoder and decoder. As discussed above, context model including h_a, h_s is also entropy-constrained. However increasing the parameters of context model facilitate the compression performance, especially for high bit-rate. Since the range of y^o has become large, the value of v or the output of context model has more probabilities. Thus the capability of h_a, h_s must adopt more varieties. Then enlarging the context model is to accurately model the distribution of y^o .

As shown in Tab. 4 GFLOPS², the performance of bpp-psnr improves as the proportion of context parameters increases. However, when the proportion of context parameters continues to increase, while the bit rate decreases, PSNR also decreases. Nevertheless, these points are located in the upper left corner of the rate-distortion curve, all belonging to the Pareto frontier.

4.4 Scaling for Dataset

To explore the compression limits on the Kodak dataset, we conducted direct overfitting on the Kodak data to investigate the boundary of PSNR. It was observed that at 0.1bpp , the PSNR can reach up to $\sim 33\text{dB}$. From the overfitting results of different structures, in which this paper obtains 34.750dB at 0.25bpp and ELIC obtains 35.526dB at 0.256bpp , it can be seen that stronger structures lead to better performance, but this phenomenon is obvious in the medium and high bit rates, while the performance of the two is close in the low bit rate. It indicates that after the input information has been quantized and screened in the low bit rate, the importance of structure and parameters decreases, but in the medium and high bit rates, the importance of structure is highlighted, and the context is more important. The overfitting of the Kodak dataset enables all parameters to be approximated as context, which greatly improves the performance.

For CLIC2021 professional dataset, the overfitting models on Kodak get much worse rate-distortion performance with 27.06dB at 0.53bpp , while the normal model with 8000 training dataset obtains 31.74dB at 0.09bpp . This indicates that the generalization of training with a limited data set has great limitations, and that compression is to match patterns in images. Since 8000 training data contains almost all common image patterns, it can effectively compress most images. It can be further illustrated that LIC is data-driven and scene-adaptive, which also provides significant data support for the customized application of LIC.

Training with mixed dataset, this does not effectively enhance the performance. The context enhancement effect brought by the Kodak dataset is diluted by the other training sets, resulting in negligible bias of the model toward the Kodak dataset alone. Besides further scaling for dataset from 8000 to 16000 images sampled from Imagenet makes a little difference for representation since the information bottleneck as shown in the left of Fig. 5. Similar with traditional compression methods, the latents y^o are orthogonal and sparse like discrete cosine coefficients. The training dataset is treated as \mathcal{X} , and \mathcal{Y} are the codebook extracted by g_a . This phenomenon also indicates that LIC attempts to learn the pattern relationships among all image pixels, with this relationship explicitly represented as context and structure in the context modeling, and implicitly represented within the model parameters.

5 Experiment

5.1 Datasets

Training dataset is 8000 images extracted from Imagenet [18] with greater than 500×500 resolution, and testing dataset is Kodak [37], CLIC 2021 professional dataset [72] and Technick dataset with 1200×1200 resolutions.

5.2 Settings

The training setting is the same as ELIC [26] except for the number of channels $M = \{240, 320, 320, 360, 360\}$ for our standard model, with $\lambda = \{2, 4, 8, 20, 35\} \times 10^{-3}$ for lower bit-rate. Then $M = \{1024, 1024, 1024, 1024\}$ for our larger model, with $\lambda = \{8, 20, 35, 50\} \times 10^{-3}$ for higher bit-rate. While 'Overfitting' experiments are the same setting with the standard models with Kodak training data. Besides the quantization step default is 0.04 for all λ . We train all models with 8000 epochs, the first 6000 epochs have learning rate with 1×10^{-4} , the remaining 2000 epochs are 1×10^{-5} .

²PyTorch profiler which calculates the flops of PyTorch operators

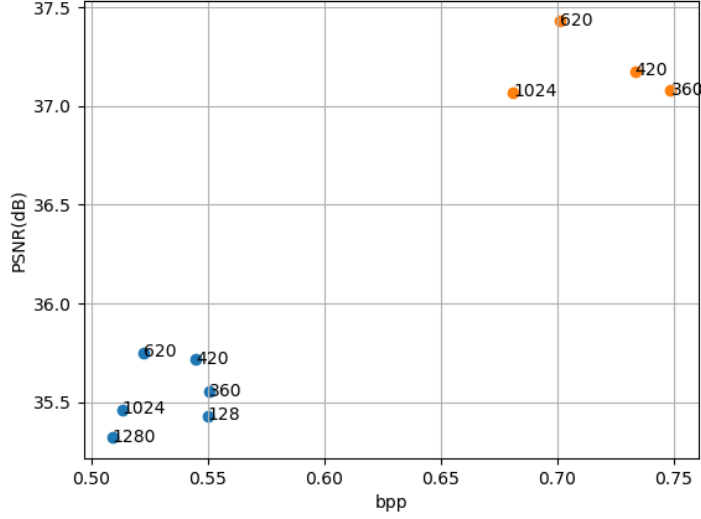


Figure 4: The rate-distortion performance with channel number of context model .

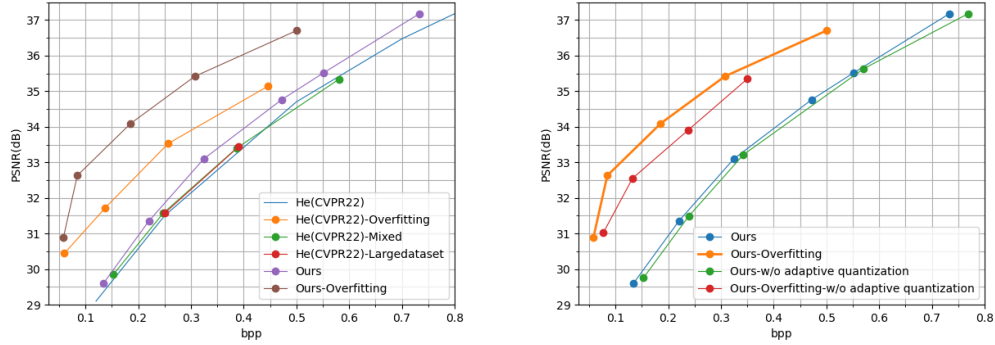


Figure 5: left:The influence of training dataset. right:The influence of adaptive quantization.

5.3 Results

As shown in Fig. 2, Fig. 3, this paper achieves the best bpp-PSNR over Kodak, CLIC2021 professional and Technick datasets. And we obtain 14.39% BD-RATE gain and 69.22% BD-PSNR gain over VVC, far higher than Liu [51].

5.4 Ablation experiments

This paper discusses the training dataset, including overfitting, using larger-scale datasets, and training with a mix of the test and training sets. The results, as shown in the left of Fig. 5, indicate that overfitting effectively enhances the context modeling capability. However, further enlarging the training dataset, even by mixing in the Kodak dataset with the training set, does not improve the compression performance on the Kodak dataset.

This paper also explores the impact of quantization as shown in the right of Fig. 5. The absence of quantization results in a decrease in PSNR, and in cases of overfitting, the PSNR decline is even more pronounced.

6 Discussion

Due to differences in network architecture and training methods, overfitting may yield varying results. This also demonstrates that this approach does not define the compression limits of LIC but rather proves that with more suitable context modeling is more efficient.

Although experiments involving simple scaling of the backbone demonstrate that further increasing the parameters does not continue to enhance compression gain in LIC, two issues need further research. First, CNN networks may not possess the scaling laws characteristics of transformers. Second, due to the smoothness and locality of images, the tokenization process differs from that of textual information and requires additional research. Besides the aforementioned entropy constraints, all these factors limit the further improvement of objective metrics of LIC.

References

- [1] Eirikur Agustsson, David Minnen, George Toderici, and Fabian Mentzer. Multi-realism image compression with a conditional generator. In *Proceedings of the IEEE/CVF Conference on Computer Vision and Pattern Recognition*, pages 22324–22333, 2023.
- [2] Eirikur Agustsson, Michael Tschannen, Fabian Mentzer, Radu Timofte, and Luc Van Gool. Generative adversarial networks for extreme learned image compression. In *Proceedings of the IEEE/CVF International Conference on Computer Vision*, pages 221–231, 2019.
- [3] Jyrki Alakuijala, Ruud van Asseldonk, Sami Boukourt, Martin Bruse, Iulia-Maria Comşa, Moritz Firsching, Thomas Fischbacher, Evgenii Kliuchnikov, Sebastian Gomez, Robert Obryk, et al. Jpeg xl next-generation image compression architecture and coding tools. In *Applications of Digital Image Processing XLII*, volume 11137, page 111370K. International Society for Optics and Photonics, 2019.
- [4] Nabajeet Barman and Maria G Martini. An evaluation of the next-generation image coding standard avif. In *2020 Twelfth International Conference on Quality of Multimedia Experience (QoMEX)*, pages 1–4. IEEE, 2020.
- [5] Fabrice Bellard. Bpg image format. URL <https://bellard.org/bpg>, 1:2, 2015.
- [6] James Betker, Gabriel Goh, Li Jing, Tim Brooks, Jianfeng Wang, Linjie Li, Long Ouyang, Juntang Zhuang, Joyce Lee, Yufei Guo, et al. Improving image generation with better captions. *Computer Science*. <https://cdn.openai.com/papers/dall-e-3.pdf>, 2(3):8, 2023.
- [7] Gisle Bjontegaard. Calculation of average psnr differences between rd-curves. *VCEG-M33*, 2001.
- [8] Yochai Blau and Tomer Michaeli. Rethinking lossy compression: The rate-distortion-perception tradeoff. In *International Conference on Machine Learning*, pages 675–685. PMLR, 2019.
- [9] Frank Bossen et al. Common test conditions and software reference configurations. *JCTVC-L1100*, 12(7):1, 2013.
- [10] Ethan Caballero, Kshitij Gupta, Irina Rish, and David Krueger. Broken neural scaling laws. *arXiv preprint arXiv:2210.14891*, 2022.
- [11] Jianrui Cai and Lei Zhang. Deep image compression with iterative non-uniform quantization. In *2018 25th IEEE International Conference on Image Processing (ICIP)*, pages 451–455. IEEE, 2018.
- [12] Lahiru D Chamain, Fabien Racapé, Jean Bégaint, Akshay Pushparaja, and Simon Feltman. End-to-end optimized image compression for machines, a study. In *2021 Data Compression Conference (DCC)*, pages 163–172. IEEE, 2021.
- [13] Tong Chen and Zhan Ma. Variable bitrate image compression with quality scaling factors. In *ICASSP 2020-2020 IEEE International Conference on Acoustics, Speech and Signal Processing (ICASSP)*, pages 2163–2167. IEEE, 2020.
- [14] Yue Chen, Debargha Murherjee, Jingning Han, Adrian Grange, Yaowu Xu, Zoe Liu, Sarah Parker, Cheng Chen, Hui Su, Urvang Joshi, et al. An overview of core coding tools in the av1 video codec. In *2018 picture coding symposium (PCS)*, pages 41–45. IEEE, 2018.
- [15] Hyomin Choi and Ivan V Bajić. Deep feature compression for collaborative object detection. In *2018 25th IEEE International Conference on Image Processing (ICIP)*, pages 3743–3747. IEEE, 2018.
- [16] Hyomin Choi, Fabien Racapé, Shahab Hamidi-Rad, Mateen Ulhaq, and Simon Feltman. Frequency-aware learned image compression for quality scalability. In *2022 IEEE International Conference on Visual Communications and Image Processing (VCIP)*, pages 1–5. IEEE, 2022.
- [17] Yoojin Choi, Mostafa El-Khamy, and Jungwon Lee. Variable rate deep image compression with a conditional autoencoder. In *Proceedings of the IEEE/CVF International Conference on Computer Vision*, pages 3146–3154, 2019.
- [18] Jia Deng, Wei Dong, Richard Socher, Li-Jia Li, Kai Li, and Li Fei-Fei. Imagenet: A large-scale hierarchical image database. In *2009 IEEE conference on computer vision and pattern recognition*, pages 248–255. Ieee, 2009.

- [19] Prafulla Dhariwal and Alexander Nichol. Diffusion models beat gans on image synthesis. *Advances in neural information processing systems*, 34:8780–8794, 2021.
- [20] Alexey Dosovitskiy, Lucas Beyer, Alexander Kolesnikov, Dirk Weissenborn, Xiaohua Zhai, Thomas Unterthiner, Mostafa Dehghani, Matthias Minderer, Georg Heigold, Sylvain Gelly, et al. An image is worth 16x16 words: Transformers for image recognition at scale. *arXiv preprint arXiv:2010.11929*, 2020.
- [21] Lingyu Duan, Jiaying Liu, Wenhan Yang, Tiejun Huang, and Wen Gao. Video coding for machines: A paradigm of collaborative compression and intelligent analytics. *IEEE Transactions on Image Processing*, 29:8680–8695, 2020.
- [22] Yimian Fang, Wen Fei, Shaohui Li, Wenrui Dai, Chenglin Li, Junni Zou, and Hongkai Xiong. Fully integerized end-to-end learned image compression. In *2023 Data Compression Conference (DCC)*, pages 337–337. IEEE, 2023.
- [23] Ruoyu Feng, Yixin Gao, Xin Jin, Runsen Feng, and Zhibo Chen. Semantically structured image compression via irregular group-based decoupling. In *Proceedings of the IEEE/CVF International Conference on Computer Vision*, pages 17237–17247, 2023.
- [24] Ge Gao, Pei You, Rong Pan, Shunyuan Han, Yuanyuan Zhang, Yuchao Dai, and Hojae Lee. Neural image compression via attentional multi-scale back projection and frequency decomposition. In *Proceedings of the IEEE/CVF International Conference on Computer Vision*, pages 14677–14686, 2021.
- [25] Zongyu Guo, Zhizheng Zhang, Runsen Feng, and Zhibo Chen. Soft then hard: Rethinking the quantization in neural image compression. In *International Conference on Machine Learning*, pages 3920–3929. PMLR, 2021.
- [26] Dailan He, Ziming Yang, Weikun Peng, Rui Ma, Hongwei Qin, and Yan Wang. Elic: Efficient learned image compression with unevenly grouped space-channel contextual adaptive coding. In *Proceedings of the IEEE/CVF Conference on Computer Vision and Pattern Recognition*, pages 5718–5727, 2022.
- [27] Dailan He, Ziming Yang, Hongjiu Yu, Tongda Xu, Jixiang Luo, Yuan Chen, Chenjian Gao, Xinjie Shi, Hongwei Qin, and Yan Wang. Po-elic: Perception-oriented efficient learned image coding. In *Proceedings of the IEEE/CVF Conference on Computer Vision and Pattern Recognition*, pages 1764–1769, 2022.
- [28] Dailan He, Yaoyan Zheng, Baocheng Sun, Yan Wang, and Hongwei Qin. Checkerboard context model for efficient learned image compression. In *Proceedings of the IEEE/CVF Conference on Computer Vision and Pattern Recognition*, pages 14771–14780, 2021.
- [29] Tom Henighan, Jared Kaplan, Mor Katz, Mark Chen, Christopher Hesse, Jacob Jackson, Heewoo Jun, Tom B Brown, Prafulla Dhariwal, Scott Gray, et al. Scaling laws for autoregressive generative modeling. *arXiv preprint arXiv:2010.14701*, 2020.
- [30] Jordan Hoffmann, Sebastian Borgeaud, Arthur Mensch, Elena Buchatskaya, Trevor Cai, Eliza Rutherford, Diego de Las Casas, Lisa Anne Hendricks, Johannes Welbl, Aidan Clark, et al. Training compute-optimal large language models. *arXiv preprint arXiv:2203.15556*, 2022.
- [31] Yueyu Hu, Shuai Yang, Wenhan Yang, Ling-Yu Duan, and Jiaying Liu. Towards coding for human and machine vision: A scalable image coding approach. In *2020 IEEE International Conference on Multimedia and Expo (ICME)*, pages 1–6. IEEE, 2020.
- [32] Khawar Islam, L Minh Dang, Sujin Lee, and Hyeonjoon Moon. Image compression with recurrent neural network and generalized divisive normalization. In *Proceedings of the IEEE/CVF Conference on Computer Vision and Pattern Recognition*, pages 1875–1879, 2021.
- [33] Afsana Ahsan Jeny, Masum Shah Junayed, and Md Baharul Islam. An efficient end-to-end image compression transformer. In *2022 IEEE International Conference on Image Processing (ICIP)*, pages 1786–1790. IEEE, 2022.
- [34] Wei Jiang, Wei Wang, Songnan Li, and Shan Liu. Online meta adaptation for variable-rate learned image compression. In *Proceedings of the IEEE/CVF Conference on Computer Vision and Pattern Recognition*, pages 498–506, 2022.
- [35] Chia-Hao Kao, Ying-Chieh Weng, Yi-Hsin Chen, Wei-Chen Chiu, and Wen-Hsiao Peng. Transformer-based variable-rate image compression with region-of-interest control. In *2023 IEEE International Conference on Image Processing (ICIP)*, pages 2960–2964. IEEE, 2023.
- [36] Maxime Kawawa-Beaudan, Ryan Roggenkemper, and Avidesh Zakhor. Recognition-aware learned image compression. *arXiv preprint arXiv:2202.00198*, 2022.
- [37] Eastman Kodak. Kodak lossless true color image suite (photocd pcd0992), 1993. URL <http://r0k.us/graphics/kodak>, 10, 2022.
- [38] Shinobu Kudo, Yukihiko Bandoh, Seishi Takamura, and Masaki Kitahara. Lvq-vae: End-to-end hyperprior-based variational image compression with lattice vector quantization. *OpenReview*:<https://openreview.net/pdf?id=1pGmKJvneD7>, 2022.
- [39] Jani Lainema, Miska M Hannuksela, Vinod K Malamal Vadakital, and Emre B Aksu. Hevc still image coding and high efficiency image file format. In *2016 IEEE International Conference on Image Processing (ICIP)*, pages 71–75. IEEE, 2016.
- [40] Nam Le, Honglei Zhang, Francesco Cricri, Ramin Ghaznavi-Youvalari, and Esa Rahtu. Image coding for machines: an end-to-end learned approach. In *ICASSP 2021-2021 IEEE International Conference on Acoustics, Speech and Signal Processing (ICASSP)*, pages 1590–1594. IEEE, 2021.

- [41] Nam Le, Honglei Zhang, Francesco Cricri, Ramin Ghaznavi-Youvalari, Hamed Rezazadegan Tavakoli, and Esa Rahtu. Learned image coding for machines: A content-adaptive approach. In *2021 IEEE International Conference on Multimedia and Expo (ICME)*, pages 1–6. IEEE, 2021.
- [42] Jooyoung Lee, Seunghyun Cho, and Seung-Kwon Beack. Context-adaptive entropy model for end-to-end optimized image compression. *arXiv preprint arXiv:1809.10452*, 2019.
- [43] Jooyoung Lee, Seyoon Jeong, and Munchurl Kim. Selective compression learning of latent representations for variable-rate image compression. *Advances in Neural Information Processing Systems*, 35:13146–13157, 2022.
- [44] Chongxin Li, Jixiang Luo, Wenrui Dai, Chenglin Li, Junni Zou, and Hongkai Xiong. Spatial-channel context-based entropy modeling for end-to-end optimized image compression. In *2020 IEEE International Conference on Visual Communications and Image Processing (VCIP)*, pages 222–225. IEEE, 2020.
- [45] Han Li, Shaohui Li, Wenrui Dai, Chenglin Li, Junni Zou, and Hongkai Xiong. Frequency-aware transformer for learned image compression. *arXiv preprint arXiv:2310.16387*, 2023.
- [46] Jiahao Li, Bin Li, and Yan Lu. Neural video compression with feature modulation. *arXiv preprint arXiv:2402.17414*, 2024.
- [47] Mu Li, Kede Ma, Jane You, David Zhang, and Wangmeng Zuo. Efficient and effective context-based convolutional entropy modeling for image compression. *IEEE Transactions on Image Processing*, 29:5900–5911, 2020.
- [48] Liewen Liao, Shaohui Li, Jixiang Luo, Wenrui Dai, Chenglin Li, Junni Zou, and Hongkai Xiong. Efficient decoder for learned image compression via structured pruning. In *2022 Data Compression Conference (DCC)*, pages 464–464. IEEE, 2022.
- [49] Chaoyi Lin, Jiabao Yao, Fangdong Chen, and Li Wang. A spatial rnn codec for end-to-end image compression. In *Proceedings of the IEEE/CVF Conference on Computer Vision and Pattern Recognition*, pages 13269–13277, 2020.
- [50] JHC Lisman and MCA Van Zuylén. Note on the generation of most probable frequency distributions. *Statistica Neerlandica*, 26(1):19–23, 1972.
- [51] Jinming Liu, Heming Sun, and Jiro Katto. Learned image compression with mixed transformer-cnn architectures. In *Proceedings of the IEEE/CVF Conference on Computer Vision and Pattern Recognition*, pages 14388–14397, 2023.
- [52] Zhiyuan Liu, Lili Meng, Yanyan Tan, Jia Zhang, and Huaxiang Zhang. Image compression based on octave convolution and semantic segmentation. *Knowledge-Based Systems*, 228:107254, 2021.
- [53] Ming Lu, Peiyao Guo, Huiqing Shi, Chuntong Cao, and Zhan Ma. Transformer-based image compression. *arXiv preprint arXiv:2111.06707*, 2021.
- [54] Jixiang Luo. Compressible and searchable: Ai-native multi-modal retrieval system with learned image compression. *arXiv preprint arXiv:2404.10234*, 2024.
- [55] Jixiang Luo, Shaohui Li, Wenrui Dai, Yuhui Xu, De Cheng, Gang Li, and Hongkai Xiong. Noise-to-compression variational autoencoder for efficient end-to-end optimized image coding. In *2020 Data Compression Conference (DCC)*, pages 33–42. IEEE, 2020.
- [56] Jixiang Luo, Yan Wang, and Hongwei Qin. Super-high-fidelity image compression via hierarchical-roi and adaptive quantization. *arXiv preprint arXiv:2403.13030*, 2024.
- [57] Fabian Mentzer, George D Toderici, Michael Tschannen, and Eirikur Agustsson. High-fidelity generative image compression. *Advances in Neural Information Processing Systems*, 33:11913–11924, 2020.
- [58] David Minnen, Johannes Ballé, and George Toderici. Joint autoregressive and hierarchical priors for learned image compression. *arXiv preprint arXiv:1809.02736*, 2018.
- [59] David Minnen and Saurabh Singh. Channel-wise autoregressive entropy models for learned image compression. In *2020 IEEE International Conference on Image Processing (ICIP)*, pages 3339–3343. IEEE, 2020.
- [60] Sung Y Park and Anil K Bera. Maximum entropy autoregressive conditional heteroskedasticity model. *Journal of Econometrics*, 150(2):219–230, 2009.
- [61] Yash Patel, Srikanth Appalaraju, and R Manmatha. Saliency driven perceptual image compression. In *Proceedings of the IEEE/CVF Winter Conference on Applications of Computer Vision*, pages 227–236, 2021.
- [62] Robin Rombach, Andreas Blattmann, Dominik Lorenz, Patrick Esser, and Björn Ommer. High-resolution image synthesis with latent diffusion models. In *Proceedings of the IEEE/CVF conference on computer vision and pattern recognition*, pages 10684–10695, 2022.
- [63] Junqi Shi, Ming Lu, and Zhan Ma. Rate-distortion optimized post-training quantization for learned image compression. *IEEE Transactions on Circuits and Systems for Video Technology*, 2023.
- [64] Zhanjun Si and Ke Shen. Research on the webp image format. In *Advanced graphic communications, packaging technology and materials*, pages 271–277. Springer, 2016.
- [65] Myungseo Song, Jinyoung Choi, and Bohyung Han. Variable-rate deep image compression through spatially-adaptive feature transform. In *Proceedings of the IEEE/CVF International Conference on Computer Vision*, pages 2380–2389, 2021.

- [66] Heming Sun, Zhengxue Cheng, Masaru Takeuchi, and Jiro Katto. End-to-end learned image compression with fixed point weight quantization. In *2020 IEEE International Conference on Image Processing (ICIP)*, pages 3359–3363. IEEE, 2020.
- [67] Heming Sun, Lu Yu, and Jiro Katto. Improving latent quantization of learned image compression with gradient scaling. In *2022 IEEE International Conference on Visual Communications and Image Processing (VCIP)*, pages 1–5. IEEE, 2022.
- [68] Heming Sun, Lu Yu, and Jiro Katto. Q-lic: Quantizing learned image compression with channel splitting. *IEEE Transactions on Circuits and Systems for Video Technology*, 2022.
- [69] Simeng Sun, Tianyu He, and Zhibo Chen. Semantic structured image coding framework for multiple intelligent applications. *IEEE Transactions on Circuits and Systems for Video Technology*, 31(9):3631–3642, 2020.
- [70] Zhenhong Sun, Zhiyu Tan, Xiuyu Sun, Fangyi Zhang, Yichen Qian, Dongyang Li, and Hao Li. Interpolation variable rate image compression. In *Proceedings of the 29th ACM international conference on multimedia*, pages 5574–5582, 2021.
- [71] Vivienne Sze, Madhukar Budagavi, and Gary J Sullivan. High efficiency video coding (hevc). In *Integrated circuit and systems, algorithms and architectures*, volume 39, page 40. Springer, 2014.
- [72] Lucas Theis and George Toderici. Clic, workshop and challenge on learned image compression. *URL <https://clic.compression.cc/2021/tasks/index.html>*, 2021.
- [73] George Toderici, Sean M O’Malley, Sung Jin Hwang, Damien Vincent, David Minnen, Shumeet Baluja, Michele Covell, and Rahul Sukthankar. Variable rate image compression with recurrent neural networks. *arXiv preprint arXiv:1511.06085*, 2015.
- [74] George Toderici, Damien Vincent, Nick Johnston, Sung Jin Hwang, David Minnen, Joel Shor, and Michele Covell. Full resolution image compression with recurrent neural networks. In *Proceedings of the IEEE conference on Computer Vision and Pattern Recognition*, pages 5306–5314, 2017.
- [75] Ties van Rozendaal, Tushar Singhal, Hoang Le, Guillaume Sautiere, Amir Said, Krishna Buska, Anjuman Raha, Dimitris Kalatzis, Hitarth Mehta, Frank Mayer, et al. Mobilencv: Real-time 1080p neural video compression on a mobile device. In *Proceedings of the IEEE/CVF Winter Conference on Applications of Computer Vision*, pages 4323–4333, 2024.
- [76] Gregory K Wallace. The jpeg still picture compression standard. *IEEE transactions on consumer electronics*, 38(1):xviii–xxxiv, 1992.
- [77] Meng Wang, Kai Zhang, Li Zhang, Yue Li, Junru Li, Yue Wang, and Shiqi Wang. End-to-end image compression with swin-transformer. In *2022 IEEE International Conference on Visual Communications and Image Processing (VCIP)*, pages 1–5. IEEE, 2022.
- [78] Jiahong Xiao, Lavisha Aggarwal, Prithviraj Banerjee, Manoj Aggarwal, and Gerard Medioni. Identity preserving loss for learned image compression. In *Proceedings of the IEEE/CVF Conference on Computer Vision and Pattern Recognition*, pages 517–526, 2022.
- [79] Sang Michael Xie, Aditi Raghunathan, Percy Liang, and Tengyu Ma. An explanation of in-context learning as implicit bayesian inference. *arXiv preprint arXiv:2111.02080*, 2021.
- [80] Hongjiu Yu, Qiancheng Sun, Jin Hu, Xingyuan Xue, Jixiang Luo, Dailan He, Yilong Li, Pengbo Wang, Yuanyuan Wang, Yaxu Dai, et al. Evaluating the practicality of learned image compression. *arXiv preprint arXiv:2207.14524*, 2022.
- [81] Liang Yuan, Jixiang Luo, Shaohui Li, Wenrui Dai, Chenglin Li, Junni Zou, and Hongkai Xiong. Learned image compression with channel-wise grouped context modeling. In *2021 IEEE International Conference on Image Processing (ICIP)*, pages 2099–2103. IEEE, 2021.
- [82] Xi Zhang and Xiaolin Wu. Lvqac: Lattice vector quantization coupled with spatially adaptive companding for efficient learned image compression. In *Proceedings of the IEEE/CVF Conference on Computer Vision and Pattern Recognition*, pages 10239–10248, 2023.
- [83] Yuefeng Zhang and Kai Lin. End-to-end optimized image compression with the frequency-oriented transform. *Machine Vision and Applications*, 35(2):27, 2024.
- [84] Zhisheng Zhong, Hiroaki Akutsu, and Kiyoharu Aizawa. Channel-level variable quantization network for deep image compression. *arXiv preprint arXiv:2007.12619*, 2020.